Makara Journal of Science

Volume 25
Issue 4 *December*

Article 6

12-30-2021

Magnetically Separable Fe3O4/SiO2/TiO2 Photocatalyst Composites Prepared through Hetero Agglomeration for the Photocatalytic Degradation of Paraquat

Jarnuzi Gunlazuardi
Department of Chemistry, Faculty of Mathematics and Science, University of Indonesia, Depok 16424, Indonesia, jarnuzi@ui.ac.id

Adel Fisli
Center for Technology of Nuclear Industry Materials, National Nuclear Energy Agency, Kawasan Puspiptek, Serpong 15314, Indonesia

Ridwan Ridwan
Center for Technology of Nuclear Industry Materials, National Nuclear Energy Agency, Kawasan Puspiptek, Serpong 15314, Indonesia

Yuni Krisyuningsih Krisnandi
Department of Chemistry, Faculty of Mathematics and Science, University of Indonesia, Depok 16424, Indonesia

Didier Robert
Institut de Chimie et des Procédés pour l'Energie, l'Environnement et la Santé, (UMR CNRS 7515), Université de Strasbourg, 25 rue Becquerel 67087 Strasbourg Cedex, France

Recommended Citation

Gunlazuardi, Jarnuzi; Fisli, Adel; Ridwan, Ridwan; Krisnandi, Yuni Krisyuningsih; and Robert, Didier (2021) "Magnetically Separable Fe3O4/SiO2/TiO2 Photocatalyst Composites Prepared through Hetero Agglomeration for the Photocatalytic Degradation of Paraquat," *Makara Journal of Science*: Vol. 25 : Iss. 4 , Article 6.
DOI: 10.7454/mss.v25i4.1277
Available at: https://scholarhub.ui.ac.id/science/vol25/iss4/6

Makara Journal of Science, 25/4 (2021), 236–246
doi: 10.7454/mss.v25i4.1277

Magnetically Separable $Fe_3O_4/SiO_2/TiO_2$ Photocatalyst Composites Prepared through Hetero Agglomeration for the Photocatalytic Degradation of Paraquat

Jarnuzi Gunlazuardi[1*], Adel Fisli[1 2], Ridwan[2], Yuni Krisyuningsih Krisnandi[1], and Didier Robert[3]

1. Department of Chemistry, Faculty of Mathematics and Science, University of Indonesia, Depok 16424, Indonesia
2. Center for Technology of Nuclear Industry Materials, National Nuclear Energy Agency, Kawasan Puspiptek, Serpong 15314, Indonesia
3. Institut de Chimie et des Procédés pour l'Energie, l'Environnement et la Santé, (UMR CNRS 7515), Université de Strasbourg, 25 rue Becquerel 67087 Strasbourg Cedex, France

[*]*E-mail: jarnuzi@ui.ac.id*

Received September 1, 2021 | Accepted December 7, 2021

Abstract

A photocatalyst supported on magnetic material allows the simple technique by using an external magnetic material to separate photocatalyst from the treated water. Thus, it is a magnetically separable nanoparticles photocatalyst (MSNP). The use of superparamagnetic nanoparticles that do not pose spontaneous magnetic moment thus could be dispersed in water and can be recollected easily by an external magnetic bar. We prepare $Fe_3O_4/SiO_2/TiO_2$ composite by hetero agglomeration of Fe_3O_4/SiO_2 and TiO_2 at a pH range of 3 to 6.2 in an aqueous slurry. The Fe_3O_4/SiO_2 was prepared *via* co-precipitation of iron (II) and iron (III) ionic solution containing ammonium hydroxide and sodium silicate. The prepared composites were characterized by XRD, TEM, FTIR, and VSM, while the photocatalytic activities were tested toward paraquat in water. Based on zeta potential values, the Fe_3O_4/SiO_2 and TiO_2 were being hetero agglomerated at pH 5 to obtain $Fe_3O_4/SiO_2/TiO_2$ composite. The XRD characterization confirmed the presence of anatase, rutile, and magnetite crystal phases. TEM images showed that the Fe_3O_4 was covered by SiO_2 and randomly attached to TiO_2. The observed FTIR peak at 940-960 cm^{-1} attributed to -Si-O-Ti- bonding mode, ensuring photocatalyst (TiO_2) adherence to the Fe_3O_4/SiO_2 cluster. The prepared $Fe_3O_4/SiO_2/TiO_2$ composite showed good photocatalytic activity for the paraquat removal and showed a good magnetic property (VSM measurement).

Keywords: composite, $Fe_3O_4/SiO_2/TiO_2$, magnetically separable photocatalyst, paraquat, photocatalyst

Introduction

Paraquat is among the most common herbicides applied for weed killer and herbage desiccant in more than 130 countries. Paraquat poisoning in humans mainly occurs via ingestion and has a mortality of 30%–70% [1, 2]. Owing to its large availability, relatively low cost, and low toxic dose, the wide usage of paraquat has received major attention since it damages the marine environment and human's wellbeing. Hence, its possible contamination to groundwater near agriculture plantations must not be neglected. Maksuk *et al.* detected paraquat in the water near the palm plantation site in Indonesia at a level of 0.01 mg/L [3], which is higher than the allowed 1 µg/L (equal to 0.001 mg/L) maximum level of paraquat in drinking water [4]. Given the function of groundwater as a natural drinking water resource in many developing countries, proper treatment to eliminate paraquat from contaminated groundwater is needed.

Photocatalysis employing semiconductor particles is a good solution to water pollution and is effective in degrading most organic pollutants in air and water [5, 6]. Among semiconductor photocatalysts, TiO_2 is the most encouraging, due to its properties, namely exceptionally photoreactive, low cost, non-toxic, and its inertness, chemically and biologically [7]. Heterogeneous photocatalysis employing titania (TiO_2) has been investigated extensively, including in the photocatalytic degradation of pesticides [8, 9] and herbicides such as paraquat [10, 11].

Nanophotocatalysts have gained great attention due to their enhanced catalytic properties [13] and high surface area facilitating broad interactions between the surface-active catalyst and treated compounds [12]. However, in the slurry system approach, nanoparticles cause difficulty in recovering the photocatalyst after use.

Photocatalysts supported on a magnetic material could be obtained by simply using an external magnetic material to

separate the photocatalyst from the treated water [14, 15]. Superparamagnetic nanoparticles are beneficial because they lack spontaneous magnetic moments and thus can be dispersed in water. When provided with a slightly magnetic field, a maximum magnetic response can be achieved to facilitate recollection using a simple magnetic bar.

The use of iron oxide superparamagnets (magnetite or maghemite) is favorable because of their low price and non-toxicity. Magnetically separable photocatalysts have been prepared using sol–gel [16] and precipitates [17]; nevertheless, these processes require a calcination step (>400 °C) that might be causing the agglomeration of particles, loss of magnetic properties, and even unwanted high-temperature chemical reaction between materials [18]. Hetero agglomeration combines magnetic materials with pre-activated TiO_2 photocatalyst and does not necessitate a calcination step.

Hetero agglomeration occurs when two oppositely charged particles join in a medium system through electrostatic interaction [19]. The surface of TiO_2 and γ-Fe_2O_3 nanoparticles can be modified using a protective lining composed of two oppositely charged poly-electrolytes [20] or grafting with 3-aminopropyl tri-ethoxy silane [21]. Opposite charges can be generated by adjusting the pH of an aqueous slurry solution containing Fe_3O_4 and TiO_2 nanoparticles because of their different iso-electrostatic points [22, 23].

The unwanted reaction might occur between titania and iron oxide during photocatalysis and produce a photo dissolution effect, which is detrimental to the photocatalytic activity of the composite [24]. This negative influence could be hindered using an insulating layer such as SiO_2 between the magnetic and photocatalytic materials [25, 26].

In this work, Fe_3O_4/SiO_2/ TiO_2 catalyst was produced by merely adjusting the pH of the aqueous media, in which the as-prepared Fe_3O_4/SiO_2 has an opposite charge to that of the pre-activated TiO_2. Fe_3O_4/SiO_2 was prepared by hydrolyzing sodium silicate in the presence of freshly prepared Fe_3O_4 nanoparticles.

This new type of magneto-photocatalyst was investigated for paraquat photodegradation in water solution and compared with two kinds of commercial nanoparticle TiO_2 photocatalysts.

Materials and Methods

Synthesis of Fe_3O_4. Fe_3O_4 nanoparticles were prepared with the co-precipitation method of Choi *et al*. [22]. In brief, 5.2 g of $FeCl_3.6H_2O$ (Merck) and 2 g of $FeCl_2.4H_2O$ (Merck) (mol ratio of Fe[III]/Fe[II] = 2:1) were dissolved in 10.3 mL of 1 N HCl, followed by the addition of 15 mL of deionized water under constant stirring. The iron salt solution was dropwise added to the 250 mL of 1.5 M ammonium hydroxide solution with intense stirring. After the reaction, the obtained Fe_3O_4 precipitate was removed from the solution using a magnetic field and re-dispersed into de-ionized water; this process was repeatedly performed until the pH of washing water became neutral. The solid produced was dried at 60 °C overnight and at 100 °C for another 2 h in an oven.

Synthesis of $Fe3O_4/SiO_2$. Fe_3O_4/SiO_2 nanoparticles were prepared using the procedure of Zhao *et al*. [27] with minor modifications. The prepared iron salt solution was dropwise added to the 250 mL of 1.5 M ammonium hydroxide solution with intense stirring. Fe_3O_4 precipitate was dropwise added with 3.2 mL sodium silicate solution (27 wt % SiO2, Aldrich), and the pH was fixed to 10 through 2 M HCl addition. The mixture was stirred intensely for 4 h and left overnight. Lastly, the obtained Fe_3O_4/SiO_2 nano-composite was removed from the solution using a magnetic field and rinsed with deionized water frequently until the pH of the washing water became neutral. The solid produced was dried at 60 °C overnight and at 100 °C for another 2 h in an oven.

Synthesis of $Fe_3O_4/SiO_2/TiO_2$. $Fe_3O_4/SiO_2/TiO_2$ nanoparticles were prepared through hetero agglomeration. The formed Fe_3O_4/SiO_2 nanocomposite was removed from the solution by a magnetic field and rinsed with deionized water frequently until the pH of the washing water became neutral. In another flask, 4.64 g of TiO_2 was dispersed into 100 mL of 0.02 M $(NH_4)2SO_4$ 0.02 M and stirred for 30 min at room temperature. Two types of TiO_2, namely, TiO_2 (mixture of anatase and rutile) nanoparticle Aldrich and TiO_2-P25 Evonik were used. The dispersed TiO2 was mixed into Fe_3O_4/SiO_2 suspension, and the pH was fixed to 5 through 1M HCl addition. The suspension was sonicated for 30 min at room temperature and centrifuged at 4000 rpm. The solid produced was dried in an oven at 60 °C overnight and at 100 °C for another 3 h.

Characterization. Composite phases were confirmed using X-ray diffractometer (XRD, XD-610, Cu-Kα source, λ= 0.154 nm, Phillip). Transmission electron microscope (TEM) images were recorded with a transmission electron microscope (JEM-1400, JEOL). Infrared (IR) spectra were measured using a Fourier transformation infrared spectroscope (FTIR) type Tensor 27 Bruker. Powdered samples of approximately 10 mg were placed on the sample holder in the FTIR device and irradiated with IR light within 500–4000 cm^{-1} wavelength. Magnetic properties were measured using a vibrating sample magnetometer Oxford type 1.2 T at room temperature. Surface area was determined using QuandraSorb SI-4-Kr/MP, Quantochrome). The surface

charges of Fe_3O_4, TiO_2, and Fe_3O_4/SiO_2 were determined using zeta potential (Zetasizer Nano-Zs, Malvern).

Evaluation of photocatalytic activity. Photocatalytic reactions were conducted on a slurry reactor system, and photocatalytic activity was studied for the degradation of paraquat solution in water. Approximately 250 mg of tested materials were dispersed into 250 mL of 20 mg/L paraquat. The suspension was stirred under a UV lamp 2 x 18 W with main radiation at 254 nm at room temperature. Paraquat concentration in water was measured by a UV-vis spectrophotometer at the wavelength of 258 nm and a certain time interval. Photocatalytic activity under UV irradiation was determined under varying experimental conditions, namely, pH range, catalyst type, and catalyst loading in the water

Results and Discussion

Crystalline phase structural characterization. Figure 1a displays the diffraction patterns of commercial TiO_2 used to prepare the magneto-photocatalyst nanocomposite. The XRD spectra of both TiO_2 samples revealed the occurrence of anatase (JCPDF file no. 21-172) and rutile JCPDF file no. 21-1276) phases. According to peak intensity observations, the rutile phase content in TiO_2 Aldrich was higher than that in TiO_2-P25 Evonik. TiO_2-P25 Evonik has a particle size of ~ 20 nm and consists of above 70% anatase with minor rutile and a small amorphous phase [28]. Meanwhile, TiO_2 nanoparticle mixture anatase and rutile Aldrich has a particle size of < 150 nm. Figure 1b shows the peaks related to Fe_3O_4 (magnetite) in the XRD spectrum, which resembles the standard diffraction pattern of magnetite (JCPDF file no. 03-0863). The crystallite size of Fe_3O_4 is estimated at 12.7 nm according to Scherrer equation and employed to the (311) plane. The XRD pattern of Fe_3O_4/SiO_2 was similar to that of Fe_3O_4, indicating the stability of the crystalline phase of Fe_3O_4 after being coated by silica. The lack of any XRD peak related to the silica crystal phase confirmed the amorphous phase of silica [29]. Magnetite, anatase, and rutile phase peaks were observed in the two magnetically separable photocatalyst (MSNP) composites ($Fe_3O_4/SiO_2/TiO_2$-Aldrich and $Fe_3O_4/SiO_2/TiO_2$-Evonik). This finding indicates the preservation of these phases that are essential for the photocatalysis and magnetic separation of composites in treated water.

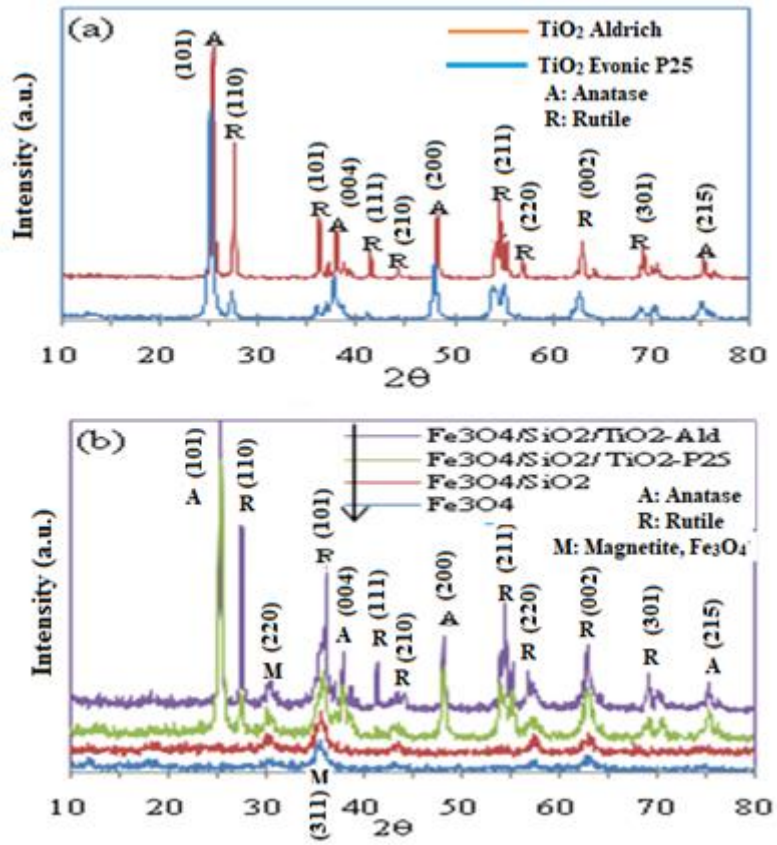

Figure 1. X-ray Diffraction Patterns of (a) TiO_2 Aldrich and TiO_2-P25-Evonik, (b) Composites and Fe_3O_4: A = Ana-tase phase, R = Rutile phase

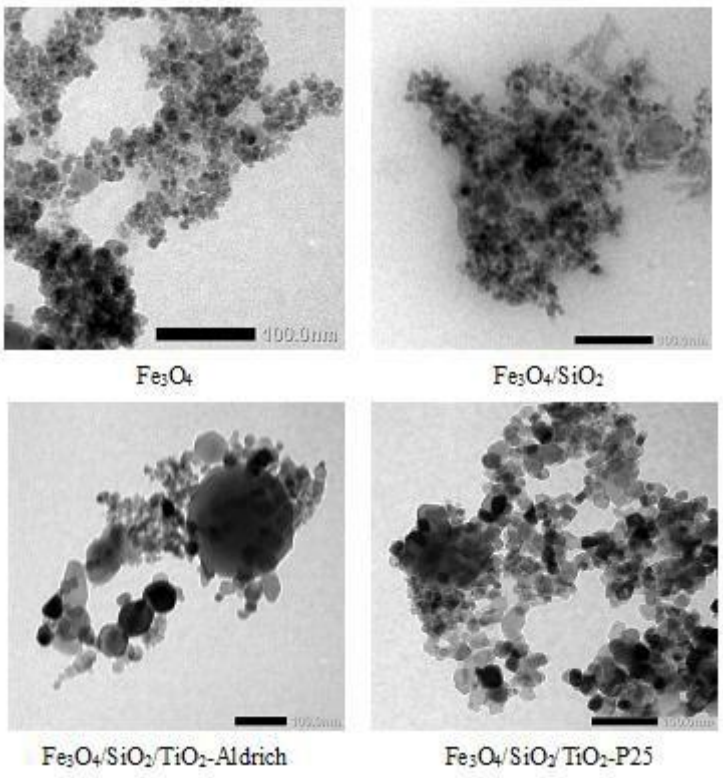

Figure 2. TEM Images of the Prepared Samples

Morphological characterization. Figure 2 reveals the TEM images of the prepared samples. The mean diameter size of Fe_3O_4 from the TEM image is less than 20 nm, that is close to the value obtained using the Scherrer formula in the XRD patterns. The magnetite particles incline to aggregate as clusters because of the magnetic dipole interaction between neighboring particles [16]. These clusters of superparamagnetic nanoparticles are beneficial for magnetic separation and retain the superparamagnetic property of the individual nanoparticles; their relatively large volume allows their effective high-gradient magnetic separation [30]. In Fe_3O_4/SiO_2, a SiO_2 coating layer (bright) covered the surface of magnetic iron oxide clusters (dark).

The TEM image of $Fe_3O_4/SiO_2/TiO_2$-Aldrich shows the difference in particle sizes between Fe_3O_4/SiO_2 and TiO_2-Aldrich. The small particles of Fe_3O_4/SiO_2 adhered on the surface of the larger particles of TiO_2-Aldrich. By comparison, the TEM image of $Fe_3O_4/SiO_2/TiO_2$-P25 shows a similar size between Fe_3O_4/SiO_2 and TiO_2-P25. Therefore, Fe_3O_4/SiO_2 and TiO_2-P25 adhered randomly and formed irregular particle clusters [31].

FTIR characterization. Figure 3 shows the FTIR spectra of Fe_3O_4/SiO_2, $Fe_3O_4/SiO_2/TiO_2$-P25, and $Fe_3O_4/SiO_2/TiO_2$-Aldrich. All curves possess a peak at ~1085 cm^{-1}, which can be assigned to the asymmetric stretching vibration of Si–O–Si. The strong peak found at 500–800 cm^{-1} corresponds to the overlapping peaks of Ti–O–Ti vibration, Si–O–Si symmetric vibration, and Fe-O stretching vibration in the crystalline lattice of Fe_3O_4. A peak assigned to the Si–O–Ti vibration was observed at 940–960 cm^{-1} [32, 33]. The availability of water was confirmed by the presence of H–O–H bending at 1630 cm^{-1} and O–H stretching at 3370 cm^{-1}. This surface hydroxylation is beneficial for the photocatalytic activity of the sample because it gives a high capacity for oxygen adsorption [34].

Magnetic and surface charge properties. Figure 4 shows the magnetic properties of Fe_3O_4 and composites determined at room temperature. Magnetization versus applied field is illustrated in the hysteresis curves. All the prepared samples possessed superparamagnetic behavior. Table 1 lists the saturation magnetization (*Ms*), remanent magnetization (*Mr*), and coercivity (*Hc*) values. The saturation magnetization value of prepared Fe_3O_4 was 57.7 emu/gr. Compounding processes reduced the saturation magnetization due to the low magnetite phase (Fe_3O_4) in the composite with a non-magnetic coating layer and due to SiO2 and TiO_2 in Fe_3O_4/SiO_2 and $Fe_3O_4/SiO_2/TiO_2$ composites, respectively. Superparamagnetic behavior was evidenced by the low values of remanent and coercivity magnetization, which can be attributed to particle aggregation during separation by an external magnetic bar. Hence,

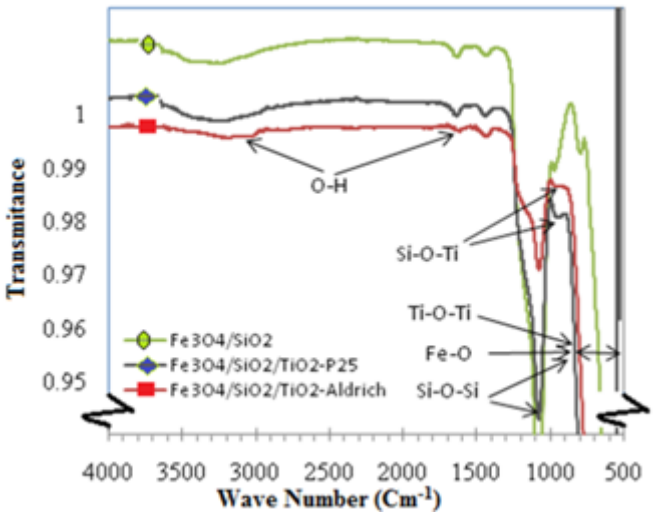

Figure 3. FTIR Spectra of Fe_3O_4/SiO_2, $Fe_3O_4/SiO_2/TiO_2$-P25-Evonik and $Fe_3O_4/SiO_2/TiO_2$-Aldrich

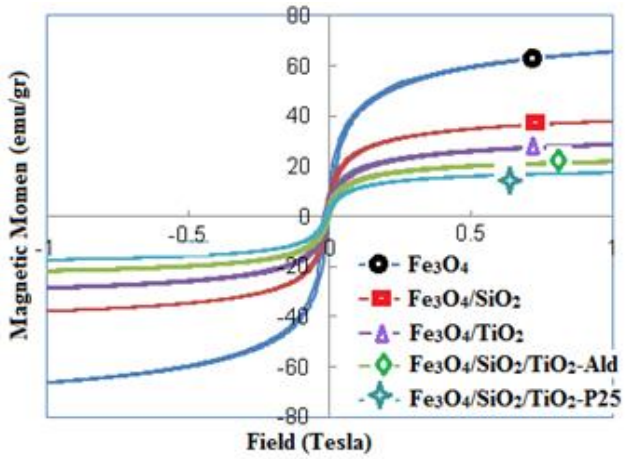

Figure 4. Magnetic Hysteresis Curve of Prepared Samples

Table 1. Saturation Magnetization, Coercivity, Remanent Magnetization, and BET Values of Prepared Magnetic and Nanocomposites

No	Sample	Saturation Magnetization (emu/gr)	Coercivity (Oe)	Remanent Magnetization (emu/gr)	BET (m^2/g)
1	Fe_3O_4	57.7	70.7	9.9	152.3
2	Fe_3O_4/SiO_2	40.7	56.5	7,8	97,52
3	Fe_3O_4/TiO_2	28.5	68.3	6.0	91.45
4	$Fe_3O_4/SiO_2/TiO_2$-Ald	21.72	61.8	4.5	53.93
5	$Fe_3O_4/SiO_2/TiO_2$-P25	17.43	62.4	3.8	86.1

the photocatalysts can be simply dispersed in a solution and recollected for recycling. Reusing the composite once and four times in repetition only slightly decreased its saturation magnetization (SI-1). Therefore, this phenomenon will not affect composite recollection in water, even after repeated usages.

Zeta potential is the surface charge derived from the magnitude of electrostatic repulsive interactions between particles in water. The iso-electric point can be found at the pH level where zeta potential is zero. Figure 5 shows the surface charge (zeta potential) of TiO_2, Fe_3O_4, and Fe_3O_4/SiO_2 determined in the pH range of 2–12. The iso-

electric point of Fe_3O_4, in which its surface charge changed from (+) to (-), occurred at pH 8. After SiO_2 was composited with Fe_3O_4 (thus Fe_3O_4/SiO_2), the iso-electric point shifted toward the acidic at pH 3. This result indicated that SiO_2 successfully coated the surface of Fe_3O_4 particles. A thin layer of SiO2 has an iso-electric point between 2.7 and 3.2 [35], and the iso-electric point of TiO_2 is at pH 6.2. At pH >3 and <6.2, Fe_3O_4/SiO_2 has a negative surface charge, whereas TiO_2 possesses a positive surface charge. Thus, the electrostatic interaction force between these two particles attracts them together. Thus, pH 5 was selected to disperse these two particles in an aqueous solution and consequently form the MSNP $Fe_3O_4/SiO_2/TiO_2$ nanocomposite.

Figure 6 shows the $Fe_3O_4/SiO_2/TiO_2$ suspension in water. The $Fe_3O_4/SiO_2/TiO_2$ formed a stable suspension in water for a long time (left). When the magnetic bar was immersed in the suspension, the $Fe_3O_4/SiO_2/TiO_2$ particles moved and attached to the surface of the magnetic bar (center). The attachment of $Fe_3O_4/SiO_2/TiO_2$ on the magnetic bar could be simply separated from water by pulling up the magnetic bar to the top of the container (right).

Photocatalytic evaluation. Photocatalytic oxidation for paraquat was conducted with a 20 ppm aqueous solution of paraquat and 1 g/L of $Fe_3O_4/SiO_2/TiO_2$ catalyst suspension under UV illumination for up to 240 min. For a specific time, the solution was subjected to UV-vis spectrometry measurement (Figure 7). Paraquat has a strong UV signal at 257 nm corresponding to π-π* transition in the pyridinium ring. Figure 8 shows that the absorption band at 257 nm decreased during irradiation time, whereas the absorption at ca. 220 nm slightly increased and then decreased because of the forming of intermediate (SI-2) and reaction products [10].

The pH of the medium plays a significant part in the adsorption and photocatalytic oxidation of pollutants [8]. Figure 9 shows the result of the photocatalytic degradation of paraquat solutions at different initial pH values Experiments with different initial pH levels were performed to investigate the influence of pH on paraquat degradation rate. Paraquat degradation was least effective at acidic pH [36]. A high pH medium effectively degraded paraquat by increasing the adsorption capacity for this chemical [10] and approaching the point of zero charge (pzc) of TiO_2. The best pH value for degradation is above the pzc point [37]. At the same pH, the prepared composite containing TiO2-P25 showed higher activity than the composite containing TiO2-Aldrich due to differences in their surface areas (Table 1). A high surface area greatly facilitates the reactions/interactions between the surface-active catalyst and the interacting media [12]. Moreover, a high anatase phase in TiO_2-P25 may lead to photocatalysis under UV irradiation [13], which may be responsible for this observation.

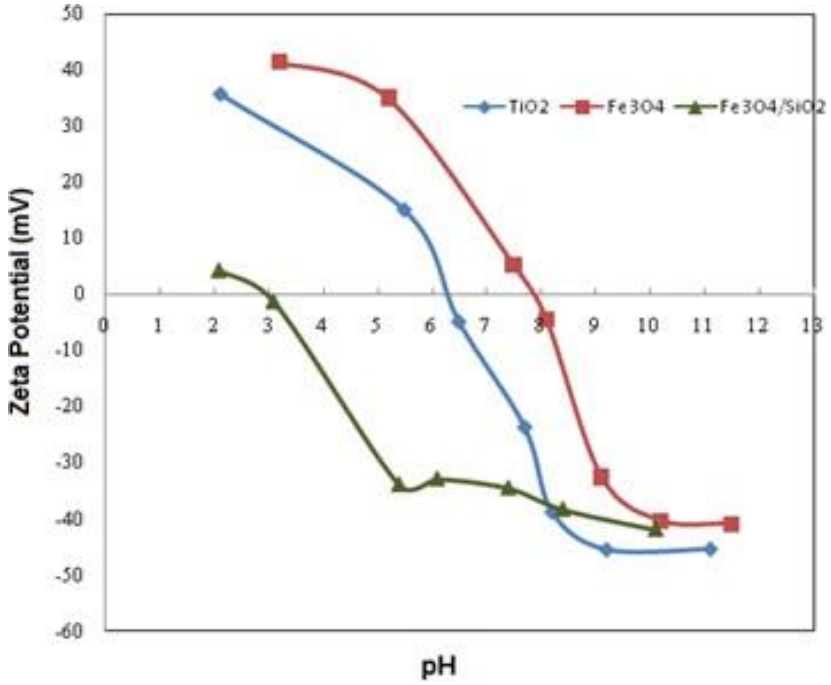

Figure 5. Zeta Potential Values of Different Materials (these are TiO_2, Fe_3O_4, and Fe_3O_4/SiO_2)

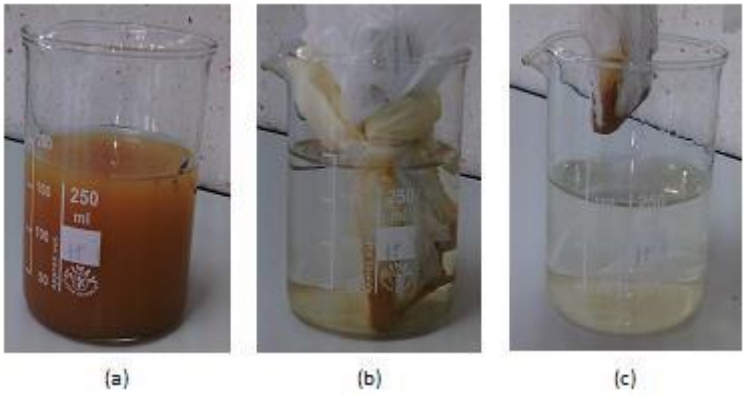

Figure 6. Illustration on the Separation of $Fe_3O_4/SiO_2/TiO_2$ in Water by External Magnetite bar. The Suspension of Nanocomposite (a), the Nanocomposite Tends to Gather on the Magnetic Bar (b) and can be Easily Recollected from The Water (c)

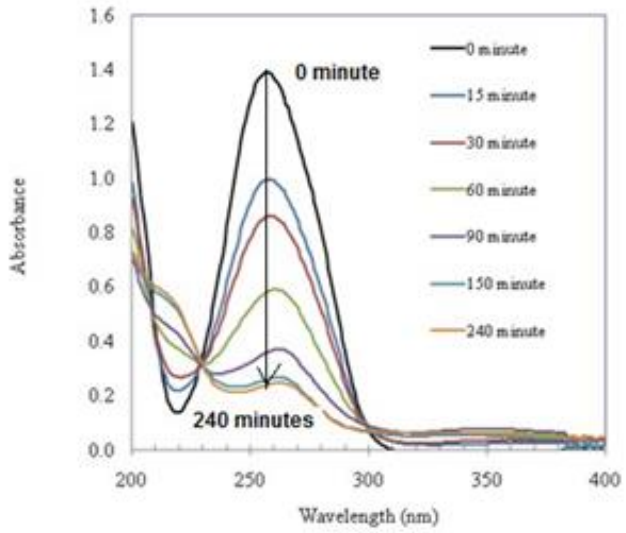

Figure 7. UV-Vis Spectra of Paraquat during Photocatalytic Experiment

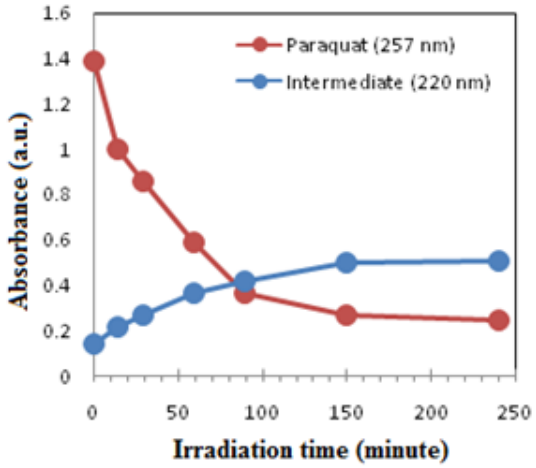

Figure 8. Absorbance Intensity of Paraquat at 220 and 257 nm during the Photocatalytic Experiment

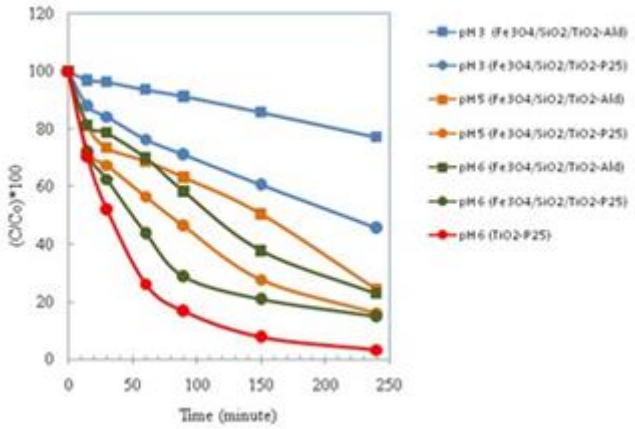

Figure 9. Photocatalytic Degradation of Paraquat in Aqueous Solution with $Fe_3O_4/SiO_2/TiO_2$- Aldrich and $Fe_3O_4/SiO_2/TiO_2$-P25 at Different Initial pH values

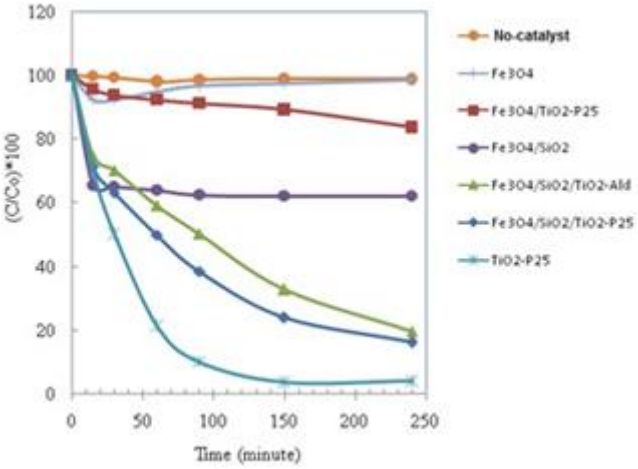

Figure 10. Photocatalytic Degradation of Paraquat in Aqueous Solution with Various Types of Photocatalysts

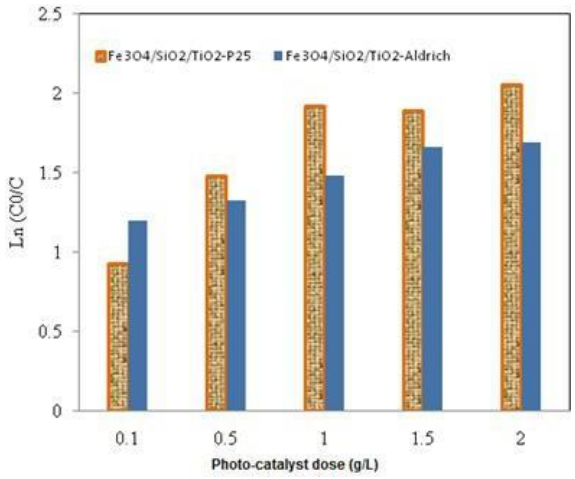

Figure 11. Comparison of Two Different Types of Prepared Photocatalysts on its dose and the Paraquat Disappearance Rate

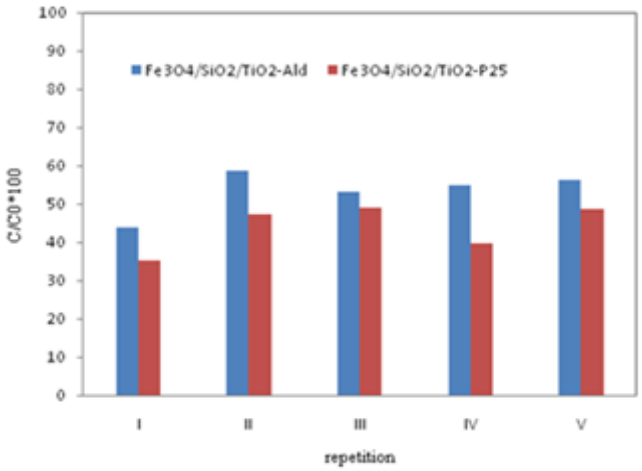

Figure 12. Recycle usage of Photocatalysts toward Degradation of Paraquat

Figure 10 shows the photocatalytic degradation of paraquat in an aqueous solution with various types of photocatalyst composites. No degradation took place during the solution was irradiated without photocatalyst and with only magnetite (Fe_3O_4). Fe_3O_4/ TiO_2 exhibited a photocatalytic effect for paraquat degradation due to TiO_2; however, its photocatalytic rate was quite low because of the photodissolution effect. This influence occurs during electronic interaction and causes charge carrier transfer across the junction between the two semiconductors in contact [24].

Photodissolution can be overcome by introducing SiO_2 as a layer between Fe_3O_4 and TiO_2 [25, 26]. In addition, SiO_2 can act as an adsorbent in the composite [38]. The presence of SiO2 in $Fe_3O_4/SiO_2/TiO_2$ composite plays a role in paraquat adsorption and may be responsible for the reduction in paraquat concentration. Amorphous silica contains silanol (groups) that has ion-exchange capabilities via the weakly acidic silanol groups [39]. The photocatalytic activity of composite dramatically intensified because of the presence of SiO_2 barrier between Fe_3O_4 and TiO_2. The synergistic influence of adsorption and photocatalytic properties was evident from the increase in paraquat removal. However, the photocatalytic activity was still lower than that of single TiO_2-P25. A single TiO_2-P25 contains only pure active material, and $Fe_3O_4/SiO_2/TiO_2$ contains non-photoactive material.

For any practical applications, the optimum loading of catalyst in wastewater treatment is necessary to prevent the catalyst's excess and assures the total absorption of efficient photons. The influence of catalyst loading in solution at 0.1–2 g/L on paraquat degradation was investigated. Figure 11 shows the relationship between catalyst loading and the first-order kinetics of paraquat. The first-order kinetics increased with catalyst loading up to 1 g/L for $Fe_3O_4/SiO_2/TiO_2$-P25 and up to 1.5 g/L for $Fe_3O_4/SiO_2/TiO_2$-Aldrich. Further increase in catalyst loading only led to a minor increase in the first-order kinetics of paraquat. However, the excessive particle loading may result in solution turbidity, thus causing the shading effect. Hence, the light transmission through the solution will be non-uniform and even reduced [40].

Photocatalyst reusability is a key point for practical applications, e.g., economically attractive. The reusability of the prepared catalysts for paraquat degradation is displayed in Figure 12. $Fe_3O_4/SiO_2/TiO_2$-P25 and $Fe_3O_4/SiO_2/TiO_2$-Aldrich particles in paraquat solution were repeatedly used for five cycles under UV irradiation for 90 min. The photocatalyst maintained a stable performance up to five cycles. For approximately 3 hrs, the photocatalyst eliminated 16 mg of paraquat per 1 L of treated water (equal to 5.3 mg/h/L) (Figure 10), and its activity almost remained the same after being used for at least five cycles (Figure 12).

Conclusion

A MSNP $Fe_3O_4/SiO_2/TiO_2$ system was successfully prepared through hetero agglomeration and showed a good photocatalytic activity while maintaining its magnetic properties. This feature facilitates easy recollection by an external magnetic bar from the treated water after use. Thus, the new $Fe_3O_4/SiO_2/TiO_2$ composite system is a potential candidate for a photocatalytic slurry reactor with a simple recollection system. The MSNP composite prepared using P-25 Evonik has more photocatalytic activity than that prepared with TiO_2 Aldrich. The $Fe_3O_4/SiO_2/TiO_2$ composite can degrade paraquat in water (5.3 mg/hr/L) under acidic conditions ($pH \leq 6$) and is retrieved with ease from treated water with almost the same activity using an external magnetic bar.

Acknowledgements

The authors gratefully acknowledge the support from DGHE, Directorate General of Higher Education, the

Republic of Indonesia under program bilateral collaboration "Hibah Kolaborasi Luar Negeri (HKLN);" and Universitas Indonesia Research Cluster Program for Titania Photo Electrocatalysis (TiPEC), and Doctoral Research Support Grant No: 1864/UN2.R12/ HKP.05.00/2015; and NKB-319/UN2.RST/HKP.05.00/ 2021. The Scholarship support from The State Ministry of Research and Technology (SMRT), Republic of Indonesia, for A.F. is also acknowledged.

Authors' Contributions

J.G. and D.R. have designed and managed the study. J.G., A.F., and YKK have written the paper. A.F. conducted the experiments. A.F. and R have measured magnetic properties and written the results. A.F. and YKK analyzed the XRD and wrote the results. All authors read and approved the final manuscript.

References

[1] Watts, M. 2011. Paraquat, Pesticide Action Network Asia & the Pacific (PANAP), pp. 1–43.

[2] Eisler, R. 1990. Paraquat Hazards to Fish, wildlife and invertebrates: A synoptic Review, U.S. Fish and Wildlife Service, Patuxent Wildlife Research Center, pp 3–38.

[3] Maksuk, T.M., Suheryanto, U.A. 2016. Environmental Health Risk Analysis of Paraquat Exposure in Palm Oil Plantations. Int. J. Pub. Health Sci. 5(4): 465–469, http://doi.org/10.11591/ijphs.v5i4. 4852.

[4] Hamilton, D.J., Ambrus, Á., Dieterle, R.M., Felsot, A.S., Harris, C.A., Holland, P.T., Katayama, A., Kurihara, N., Linders, J., Unsworth, J., Wong, S.-S. 2003. Regulatory Limits for Pesticide Residues in Water. Pure Appl. Chem. 75(8): 1123–1155.

[5] Ollis, D.F. 2000. Photocatalytic purification and remediation of contaminated air and water, Comptes Rendus de l'Académie des Sciences - Series IIC – Chemistry. Surf. Chem. Catal. 3(6): 405–411, https://doi.org/10.1016/S1387-1609(00)01169-5.

[6] Robert, D., Malato, S. 2002. Solar photocatalysis: a clean process for water detoxification. Sci. Total. Environ. 291: 85–97, https://doi.org/10.1016/S00 48-9697(01)01094-4.

[7] Friedmann, D., Mendive, C., Bahnemann, D. 2010. TiO_2 for water treatment: Parameters affecting the kinetics and mechanisms of photocatalysis. Appl. Catal. B Environ. 99: 398–406. https://doi.org/ 10.10 16/j.apcatb.2010.05.014.

[8] Ahmed, S., Rasul, M.G., Brown, R., Hashib, M.A. 2011. Influence of parameter on the heterogeneous photocatalytic degradation of pesticides and phenolic contaminants in wastewater: A short review. J. Environ. Manag. 92: 311–330, https://doi.org/ 10.1 016/j.jenvman.2010.08.028.

[9] Gunlazuardi, J., Andayani, W. 2005. Photocatalytic degradation of pentachlorphenol in aqueous solution employing immobilised TiO2 supported on titanium metal. J. Photochem. Photobiol. A Chem. 173: 51–55, https://doi.org/10.1016/j.jphotochem. 2005.01.0 02.

[10] Florencio, M.H., Pires, E., Castro, A.L., Nunes, M.R., Borges, C., Costa, F.M. 2004. Photodegradation of Diquat and Paraquat in aqueous solution by titanium dioxide: evaluation of degradation reactions and characterization of intermediates. Chemosphere. 55: 345–355, https://doi.org/10.1016/ j.chemosphere.2003.11.013.

[11] Cantavenera, M.J., Catanzaro, I., Loddo, V. 2007. Photocatalytic degradation of paraquat and genotoxicity of its intermediate products. J. Photochem. Photobiol. A Chem. 185: 277–282, https://doi.org/10.1016/j.jphotochem.2006.06.021.

[12] Chen, X., Mao, S.S. 2007. Titanium Dioxide nanomaterials: synthesis, properties, modification, and application. Chem. Rev. 107: 2891–2959, https://doi.org/10.1021/cr0500535.

[13] Macwan, D.P., Dove, P.N., Chaturvedi, S.A. 2011. Review on nano-TiO2 Sol-gel type syntheses and its application. J. Mater. Sci. 46: 3669–3686, https://doi.org/10.1007/s10853-011-5378-y.

[14] Ambashta, R.D., Sillanpaa, M. 2010. Water purification using magnetic assistance: A review. J. Hazardous Mater. 180: 38–49, https://doi.org/10.10 16/j.jhazmat.2010.04.105.

[15] Polshetiwar, V., Luque, R., Fihri, A., Zhu, H., Bouhrara, M., Basset, J.M. 2011. Magnetically Recoverable Nanocatalysts. Chem. Rev. 111: 3036–3075, https://doi.org/10.1021/cr100230z.

[16] Álvareza, P.M., Jaramillo, J., López-Pi˜nero, F., Plucinski, P.K. 2010. Preparation and characterization of magnetic TiO2 nanoparticles and their utilization for the degradation of emerging pollutants in water. Appl. Catal. B Environ. 100: 338–345, https://doi.org/10.1016/j.apcatb.2010.08.010.

[17] Tyrpekl, V., Vejpravova, J.P., Roca, A.G., Murafa, N., Szatmary, L., Niznansky, D. 2011. Magnetically Separable Photocatalytic Composite g-Fe_2O_3@TiO_2 synthesized by heterogeneous precipitation. Appl. Surf. Sci. 257, 11: 4844–4848. https://doi.org/10.1016/j.apsusc.2010.12.110.

[18] Makovec, D., Sajko, M., Selisnik, A., Drofenik, M. 2012. Low-temperature synthesis of magnetically recoverable, superparamagnetic, photocatalytic, nanocomposite particles. Mater. Chem. Phys. 136: 230–240.

[19] Cerbelaud, C., Videcoq, A., Abelard, P., Ferrando, R. 2009. Simulation of the heteroagglomeration between highly size-asymmetric ceramic particles. J. Coll. Inter. Sci. 332: 360–365, https://doi.org/ 10.1016/j.jcis.2008.11.063.

[20] Belessi,V., Lambropoulou, D., Konstantinou, I., Zboril, R., Tucek, J., Jancik, D., Albanis, T., Petridis, D. 2009. Structure and photocatalytic performance of magnetically separable titania

photocatalysts for the degradation of propachlor. Appl. Catal. B Environ. 87: 181–189, https://doi.org/10.1016/j.apcatb.2008.09.012.

[21] Makovec, D., Sajko, M., Selisnik, A., Drofenic, M. 2011. Magnetically Recoverable Photocatalytic Nanocomposite Particles for Water Treatment. Mater. Chem. Phys. 129: 83–89, https://doi.org/10.1016/j.matchemphys.2011.03.059.

[22] Choi, J.S., Youn, H.K., Kwak, B.H., Wang, Q., Yang, K.S., Chung, J.S. 2009. Preparation and characterization of TiO_2-masked Fe_3O_4 nano particles for enhancing catalytic combustion of 1,2-dichlorobenzene and incineration of polymer wastes. Appl. Catal. B Environ. 9: 210–216, https://doi.org/10.1016/j.apcatb.2009.05.026.

[23] Fisli, A., Saridewi, R, Dewi, S. H., Gunlazuardi, J. 2013. Preparation and Characterization of Fe_3O_4/TiO_2 Composites by Heteroagglomeration. Adv. Mater. Res. 626: 131–137, https://doi.org/10.4028/www.scientific.net/AMR.626.131.

[24] Beydoun, D., Amal, R., Low, G., McEvoy, S. 2002. Occurrence and Prevention of Photodissolution at the Phase Juction of Magnetite and Titanium Dioxide. J. Catal. A Chem. 180: 193–200, https://doi.org/10.1016/S1381-1169(01)00429-0.

[25] Gad-Allah, T.A., Kato, S. Satokawa, T. Kojima, 2009. Treatment of Synthetic Dyes Wastewater Utilizing a Magnetically Separable Photocatalyst ($TiO_2/SiO_2/Fe_3O_4$): Parametric and kinetic studies, Desalin. 244: 1–11. https://doi.org/10.1016/j.desal.2008.04.031.

[26] Liu, H., Jia, Z., Ji, S., Zheng, Y., Li, M., Yang, H. 2011. Synthesis of $TiO_2/SiO_2@Fe_3O_4$ Magnetic microsphere and their properties of photocatalytic degradation dyestuff. Catal. Today. 175: 293–298, https://doi.org/10.1016/j.cattod.2011.04.042.

[27] Zhao, X., Y. Shi, T. Wang, Y. Cai, G. Jiang, 2008. Preparation of silica-magnetite nanoparticle mixing hemimicelle sorbents for extraction of several typical phenolic compounds from environmental water samples. J. Chromatogr. A. 1188: 140–147, https://doi.org/10.1016/j.chroma.2008.02.069.

[28] Ohtani, B., Prieto-Mahaney, O.O., Li, D., Abe, R. 2010. What is Degussa (Evonik) P25? Crystalline composition analysis, reconstruction from isolated pure particles and photocatalytic activity test. J. Photochem. Photobiol. A Chem. 216: 179–182, https://doi.org/10.1016/j.jphotochem.2010.07.024.

[29] Emadi, M., Shams, E., Amini, M.K. 2013. Removal of Zinc from Aqueous Solutions by Magnetite Silica Core-Shell Nanoparticles. J. Chem. 787682: 1–10, https://doi.org/10.1155/2013/787682.

[30] Ditsch, A., Laibinis, P.E., Wang, D.I.C., Hatton, T.A. 2005. Controlled clustering and Enhanced Stability of Polymer-coated Magnetic Nanoparticles. Langmuir. 21: 6006–6018, https://doi.org/10.1021/la047057+.

[31] Islam, A.M., Chowdhhry, B.Z., Snowden, M.J. 1995. Heteroaggregation in colloidal dispersions. Adv. Coll. Inf. Sci. 62: 109–136, https://doi.org/10.1016/0001-8686(95)00276-V.

[32] Bousse L., Mostarshed, S., Shoot, B.V.D., De Rooij, N.F., Gimmel, P., Göpel, W. 1991. Zeta Potential Measurements of Ta_2O_5 and SiO_2 Thin Films. J. Coll. Inf. Sci. 147: 22–32, https://doi.org/10.1016/0021-9797(91)90130-Z.

[33] Shao, G.N., Elineema, G., Quang, D.V., Kim, Y.N., Shim, Y.H. 2012. Two step synthesis of a mesoporous titania-silicacomposite from titanium Oxychloride and Sodium Silicate. Pow. Technol. 217: 489–496, https://doi.org/10.1016/j.powtec. 2011.11.008.

[34] Wang, R., Wang, X., Xi, X., Hu, R., Jiang, G. 2012. Preparation and Photocatalytic Activity of Magnetic $Fe_3O_4/SiO_2/TiO_2$ composites. Adv. Mater. Sci. Eng. 409379: 1–8, https://doi.org/10.1155/ 2012/409379.

[35] Linsebigler, L.A., Lu, G., Yates, T. 1995. Photocatalysis on TiO2 surface: principles, Mechanisms, and Selected Results. Chem. Rev. 95: 735–758, https://doi.org/10.1021/cr00035a013.

[36] Gaya, U.I., Abdullah, A.H. 2008. Heterogeneous photocatalytic degradation of organic contaminant over titanium dioxide: A review of fundamentals, progress and problems. J. Photochem. Photobiol. C Photochem. Rev. 9: 1–12, https://doi.org/10.1016/j.jphotochemrev.2007.12.003.

[37] Moctezuma, E., Leyva, E., Monreal, E., Villegas, N., Infante, D. 1999. Photocatalytic degradation of the herbicide "Paraquat". Chemosphere. 39(3): 511–517, https://doi.org/10.1016/S0045-6535(98)00599-2.

[38] Fisli, A., Yusuf, S., Ridwan, S., Krisnandi Y., Gunlazuardi, J. 2014. Preparation and Characterization of Magnetite-Silica Nanocomposite as Adsorbents for Removal of Dyes from Environmental Water Samples. Adv. Mater. Res. 896: 525–531, https://doi.org/10.4028/www.scientific.net/AMR.896.525.

[39] Iller, V.R.K. 1979. The Chemistry of Silica, John Wiley & Sons, New York City: Amerika Serikat.

[40] Evgenidou, E., Bizani, E., Christophoridis, C.F. 2007. Heterogeneous photocatalytic degradation of prometryn in aqueous solution under UV-Vis irradiation. Chemosphere. 68: 1877–1882.